Article

A giant soft-shelled egg from the Late Cretaceous of Antarctica

https://doi.org/10.1038/s41586-020-2377-7

Received: 7 October 2019

Accepted: 19 March 2020

Published online: 17 June 2020

Check for updates

Lucas J. Legendre[1]✉, David Rubilar-Rogers[2], Grace M. Musser[1], Sarah N. Davis[1], Rodrigo A. Otero[3], Alexander O. Vargas[3] & Julia A. Clarke[1]✉

Egg size and structure reflect important constraints on the reproductive and life-history characteristics of vertebrates[1]. More than two-thirds of all extant amniotes lay eggs[2]. During the Mesozoic era (around 250 million to 65 million years ago), body sizes reached extremes; nevertheless, the largest known egg belongs to the only recently extinct elephant bird[3], which was roughly 66 million years younger than the last nonavian dinosaurs and giant marine reptiles. Here we report a new type of egg discovered in nearshore marine deposits from the Late Cretaceous period (roughly 68 million years ago) of Antarctica. It exceeds all nonavian dinosaur eggs in volume and differs from them in structure. Although the elephant bird egg is slightly larger, its eggshell is roughly five times thicker and shows a substantial prismatic layer and complex pore structure[4]. By contrast, the new fossil, visibly collapsed and folded, presents a thin eggshell with a layered structure that lacks a prismatic layer and distinct pores, and is similar to that of most extant lizards and snakes (Lepidosauria)[5]. The identity of the animal that laid the egg is unknown, but these preserved morphologies are consistent with the skeletal remains of mosasaurs (large marine lepidosaurs) found nearby. They are not consistent with described morphologies of dinosaur eggs of a similar size class. Phylogenetic analyses of traits for 259 lepidosaur species plus outgroups suggest that the egg belonged to an individual that was at least 7 metres long, hypothesized to be a giant marine reptile, all clades of which have previously been proposed to show live birth[6]. Such a large egg with a relatively thin eggshell may reflect derived constraints associated with body shape, reproductive investment linked with gigantism, and lepidosaurian viviparity, in which a 'vestigial' egg is laid and hatches immediately[7].

Ancestral to all mammals and reptiles including birds, the amniotic egg is diverse in size, shape and eggshell microstructure[8]. The eggshells of all Amniota possess three distinct layers: an outer calcareous layer, a proteinaceous membrana testacea, and a thinner boundary layer[5,9] (Supplementary Discussion). Microstructural features of these components have been used to assign isolated fossil eggs to major clades[4]. Most Archelosauria—dinosaurs (including birds), crocodilians and turtles—lay 'hard-shelled' eggs, in which the calcareous layer comprises most of the eggshell thickness and is organized in radially oriented prismatic structures called shell units[4,5]. By contrast, most Lepidosauria (lizards, snakes and tuatara) have a 'soft' eggshell in which the calcareous layer is reduced or absent, and the proteinaceous membrana testacea is much thicker and organized into bundles of protein fibrils[5,9]. In fossil eggs, only the thicker calcareous layer is typically preserved and the proteinaceous layers are almost never recovered[10]. The only previously known fossil reptile eggs that unambiguously lack a prismatic layer have been reported in choristoderes, the phylogenetic position of which is still unresolved[6], and in pterosaurs, among which hard-shelled eggs have also been documented[10]. Some nonavian dinosaurs have also been proposed to lack a prismatic layer[11] (Supplementary Discussion). Among fossil eggs assigned to Lepidosauria, only hard-shelled eggs have been described[4,10].

Here we identify a fossil from the Late Cretaceous (Fig. 1) as a new egg taxon. The structure of the proteinaceous layer and thin calcareous layer is consistent with a soft-shelled egg lacking a prismatic layer and pores. Computed tomography (CT) scans of the specimen show that no skeletal material is preserved inside (Supplementary Information); however, assignment to an egg taxon allows us to discuss this new egg type agnostically to the identity of the egg producer[4]. Histological thin sections, scanning electron microscopy, X-ray spectroscopy and diffraction, and mass spectrometry confirm identification of the fossil as an egg and are used to describe its microstructure and preservation, as well as its chemical and elemental composition, including its infilling sediment matrix (Fig. 1, Supplementary Methods, Supplementary Discussion and Extended Data Figs. 1–8).

[1]Department of Geological Sciences, University of Texas at Austin, Austin, TX, USA. [2]Área Paleontología, Museo Nacional de Historia Natural, Santiago, Chile. [3]Departamento de Biología, Facultad de Ciencias, Universidad de Chile, Santiago, Chile. ✉e-mail: lucasjlegendre@gmail.com; Julia_Clarke@jsg.utexas.edu

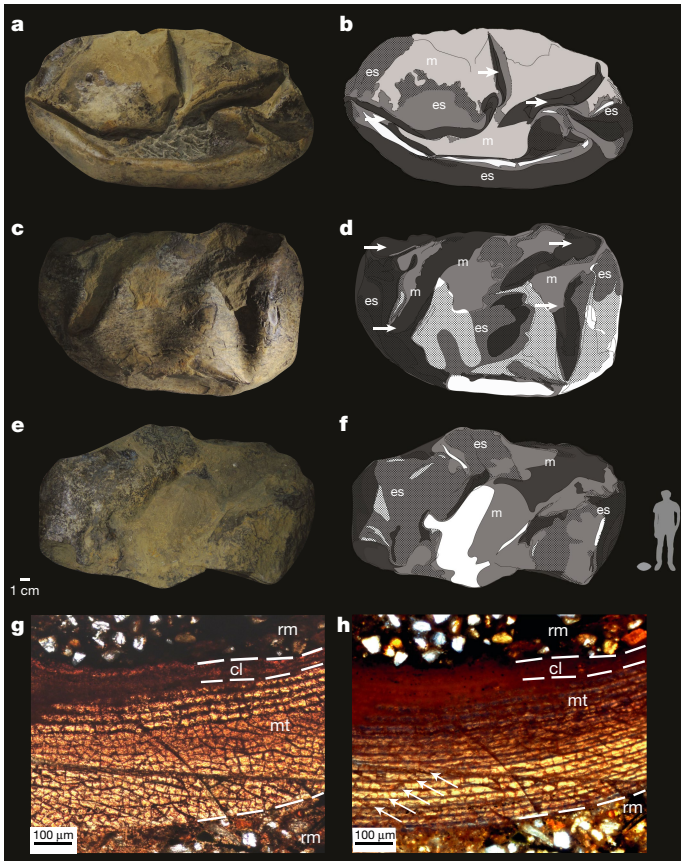

Fig. 1 | The holotype specimen of *A. bradyi*. **a**–**f**, Photographs of the holotype in lateral (**a**, **e**) and ventral (**c**) view, with corresponding line drawings (**b**, **d**, **f**). **g**, **h**, Histological section of the eggshell in plane (**g**) and cross-polarized (**h**) light. In **b**, **d**, **f**, the outer surface of the eggshell (es) is marked by large creases (arrows in **b**, **d**), within which sediment matrix (m) is visible; dashed lines indicate contacts between the sediment matrix and the preserved eggshell; and regions with eggshell fragments sampled for imaging and analyses (Extended Data Fig. 1 and Supplementary Methods) are denoted with stippling. The right insert in **f** shows the relative size of *Antarcticoolithus*. In **g**, **h**, dashed lines indicate the inferred contacts of the rock matrix (rm), calcareous layer (cl) and membrana testacea (mt). In **h**, layers in the mt are delimited by thin dark lines (arrows). The eggshell in **g**, **h** was sampled at location 3 (Extended Data Fig. 1). See Supplementary Methods, Supplementary Discussion and Extended Data Figs. 1–4.

Systematic palaeontology

Reptilia Laurenti, 1768 (sensu Modesto and Anderson, 2004)
Sauria Macartney, 1802 (sensu Rieppel and deBraga, 1996)
Oofamily, incertae sedis
Antarcticoolithus bradyi, oogen. and oospec. nov.

Etymology. *Antarctic*, referring to the continent where the specimen was discovered, Antarctica; *oolithus*, from Ancient Greek ōión for egg and líthos for stone; *bradyi*, from the Ancient Greek *bradús* for delayed or tardy, reflecting the 160 years between the description of the first Mesozoic egg from shallow marine deposits, *Testudoflexoolithus bathonicae* (Buckman, 1860)[12], and that of this new ootaxon.
Holotype. SGO.PV 25.400, an almost complete fossil egg with infilled sediment (Fig. 1), permanently reposited at the Museo Nacional de Historia Natural, Santiago, Chile.
Locality and horizon. Late Cretaceous (roughly 68 Myr) of the López de Bertodano Formation (unit Klb9; Supplementary Methods), Seymour Island, Antarctica.
Diagnosis. *Antarcticoolithus bradyi* is diagnosed by the following combination of characters: large size (29 cm × 20 cm, preserved length × width); eggshell thickness at least 700 µm and layered with a smooth undulating exterior surface; comparatively thin calcareous layer (roughly 100 µm); and complete lack of shell units and pores.
Diagnosis of the oogenus. As for the type species.

Description

Antarcticoolithus comprises the first remains of a fossil egg from Antarctica, and one of the few recovered from a marine environment[4]. It has an ovoid shape, with a 'deflated' aspect[5,13] (Fig. 1a). The eggshell as preserved is vitreous, conchoidally fractured and darker than the surrounding rock matrix (Fig. 1). It is preserved as apatite and contains isolated pyrite crystals, including framboids (Supplementary Discussion and Extended Data Figs. 2, 3)—a mineral composition found in many exceptionally preserved soft tissues[14], including the membrana testacea of fossil reptile eggs[15]. Several folds and creases are visible on all sides of the egg surface, with one side being deeply flattened (Fig. 1 and Supplementary Video), suggesting that the eggshell was originally plastic[16].

The shell contains no prismatic layer, but roughly 15 consecutive layers of approximately equal thickness (approximately 50 µm) (Fig. 1g, h and Extended Data Fig. 3a). A thin, darker outer layer (of about 100 µm), with a more granular aspect and higher calcium concentration, is identified as the calcareous layer (Fig. 1g, h and Extended Data Figs. 3, 7). This dark layer does not show any trace of erosion; however, the calcareous layer of fossil eggshells preserved as apatite is often diagenetically altered[10,15] (Supplementary Discussion). The outer and inner surface of the shell are chemically and structurally distinct from its surrounding matrix, and are similar in layered aspect and apatite composition to the fossilized proteinaceous layers of reptile eggs[5,15] (Fig. 1h, Supplementary Discussion and Extended Data Figs. 1–4, 7, 8).

To understand the scaling relationships of extant and extinct amniote eggs, including *Antarcticoolithus*, we assembled data on eggshell thickness and egg mass[10] for 148 species, encompassing every major clade (Supplementary Methods and Supplementary Table 3). We found significant allometric relationships (Fig. 2) between eggshell thickness and egg mass for both hard-shelled and soft-shelled eggs (Fig. 2a); such a relationship has not previously been described for soft-shelled eggs. The thickness of the calcareous layer differs greatly between hard-shelled and soft-shelled eggs of similar mass, with *Antarcticoolithus* falling in the latter category (Fig. 2a). Several hard-shelled eggs of birds and nonavian dinosaurs are close in size to *Antarcticoolithus* (mass = 6.5 kg), but this new specimen is the only soft-shelled egg with a mass greater than 700 g. *Antarcticoolithus* represents the largest soft-shelled egg and the second largest egg in our sample, behind that of the elephant bird *Aepyornis maximus*[3]. Conversely, its calcareous layer is extremely thin—less than one-tenth of that of similarly sized hard-shelled eggs, and one-third of that predicted for a soft-shelled egg that large (Fig. 2a). Thus, *Antarcticoolithus* is an outlier to the scaling relationships described for known amniotic eggs[3,13]. This may be due to highly specific allometric and ontogenetic constraints.

To assess how the reproductive mode and body size of the egg layer may relate to egg scaling, we assembled and phylogenetically analysed a dataset of egg measurements and body-size parameters (Supplementary Methods). Given that *Antarcticoolithus* lacks a preserved prismatic layer and plots closer to the regression for soft-shelled eggs (Fig. 2a)—comprising only lepidosaurs among extant taxa—we used egg measurements for 259 extant lepidosaur species to assess the body size of the egg layer (Fig. 2b, Supplementary Methods, Supplementary Tables 1, 2 and Extended Data Figs. 5, 6). Estimates of the snout–vent length of the egg layer are greater

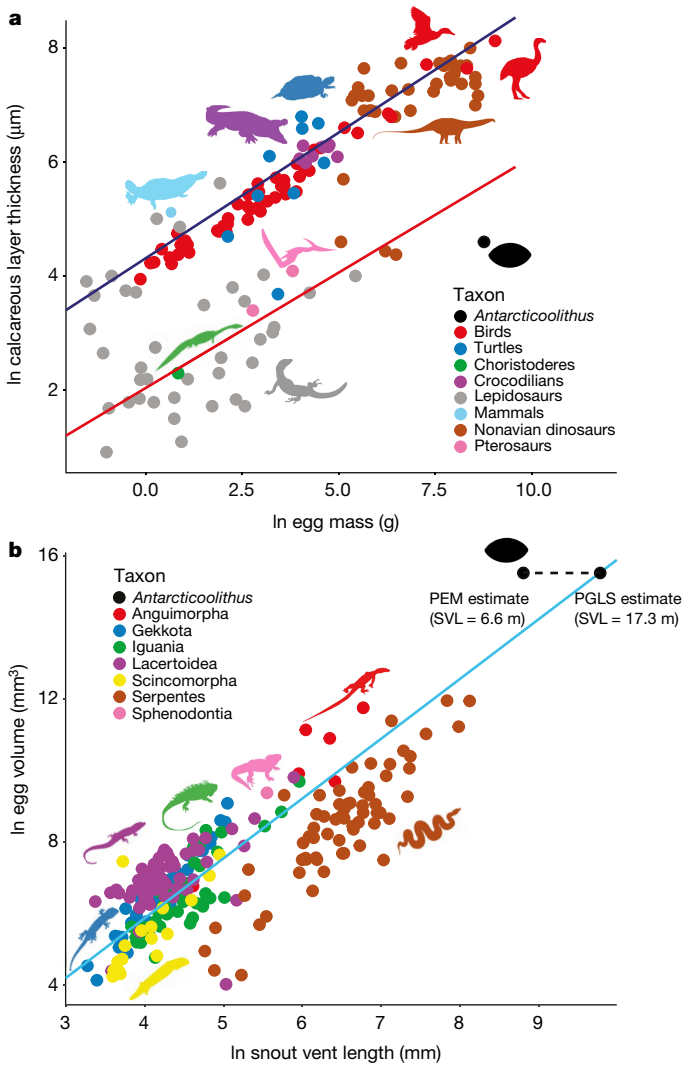

Fig. 2 | Scaling relationships of egg traits in amniotes and lepidosaurs, with *A. bradyi* pictured for comparison. a, Scaling of calcareous-layer thickness with egg mass (both log-normal) in amniotes (Supplementary Methods, dataset 2). Two regressions (phylogenetic generalized least squares (PGLS); $n = 148$) are shown for hard-shelled (blue; $r^2 = 0.8494$; $P < 2.2 \times 10^{-16}$) and soft-shelled (red; $r^2 = 0.6215$; $P = 6.899 \times 10^{-9}$) eggs. Some turtle and dinosaur eggs described as soft-shelled in the literature[10] are classified as such in this plot owing to their thin calcareous layer; nonetheless, they show a prismatic layer with shell units, not found in *Antarcticoolithus*. **b**, Scaling of egg volume with snout–vent length (SVL) in extant lepidosaurs (Supplementary Methods, dataset 1). The PGLS fit is shown ($n = 241$; $r^2 = 0.5722$; $P = 1.243 \times 10^{-13}$). For *Antarcticoolithus*, estimates of SVL from phylogenetic eigenvector map (PEM) and PGLS approaches are shown (Supplementary Methods and Discussion, Supplementary Tables 1, 3 and Extended Data Fig. 6). Select taxon silhouettes were modified from files under Public Domain licence from phylopic.org (list in the Supplementary Information).

than 6.6 m (Fig. 2b and Supplementary Methods), compatible with the more-than-10-m total body length estimates for marine reptiles that are well-represented in the Late Cretaceous of Antarctica[16]. Dinosaurs are the only amniote taxa known to lay eggs similar in mass to *Antarcticoolithus;* however, all of these largest known eggs are conspicuously hard-shelled with a thick prismatic layer, shell units and pores—all absent in *Antarcticoolithus*[4]. Much smaller nonavian dinosaur eggs have been described as soft-shelled, but still show a prismatic layer[10,11]. Although an archosaur identity cannot be ruled out (Supplementary Discussion), it would require the derived loss of morphologies that are ancestral to Archosauria and present in all largest eggs in this clade, or consistent diagenetic removal of shell units over the entire sampled surface of the egg combined with pliable folding—conditions unknown in any fossil eggs. By contrast, the structure of *Antarcticoolithus* is consistent with reproductive strategies well represented in lepidosaurs.

All viviparous lepidosaurs still lay 'vestigial' eggs that hatch in minutes to hours after oviposition; viviparity in the clade involves extended egg retention and oviposition of embryos at a late developmental stage[2,7] (Extended Data Fig. 5). Eggs associated with this strategy have a thin, poorly mineralized eggshell to increase gas exchange in utero, but a thicker eggshell is not incompatible with successful pregnancy, as other factors can facilitate gas exchange[17,18]. The relatively thick, proteinaceous eggshell of *Antarcticoolithus*, poorly mineralized and lacking pores, could thus belong to a taxon with a reproductive strategy similar to extant lepidosaur viviparity. One group of marine reptiles, mosasaurs, is recovered within the lepidosaur crown clade[19]. They, similar to sauropterygians, have been proposed to be viviparous[6] (Supplementary Discussion); however, as noted, lepidosaur viviparity is compatible with the presence of an eggshell.

The large size of *Antarcticoolithus* may be explained in part by the body size of its egg producer, but also by constraints imposed by a marine ecology. In extant soft-shelled egg layers, an increase in body size correlates with relatively smaller egg mass and larger clutch size[20,21]. Sea snakes present a notable exception, however; locomotor constraints related to their ecology have been inferred to result in a smaller clutch size[22]. Large pelagic reptiles with a streamlined body may have achieved a high reproductive investment, resulting in enlarged eggs and a smaller clutch size[22,23]—congruent with the hypothesis of some large extinct marine reptiles being K-strategists[24]. Viviparous lepidosaurs show a lower standard metabolic rate than oviparous ones, related to an increased cost of reproduction associated with extended egg retention[23]. However, large body size is known to increase the ability to maintain a high body temperature with a relatively low standard metabolic rate[25]; thus, high reproductive investment would not be incompatible with the high body temperature inferred in giant marine reptiles[26]. Such a compromise between gigantism, a streamlined body shape and viviparity may be unique to them.

In contrast to *Antarcticoolithus*, most extant amniote clades show a relatively thick eggshell for a given egg volume, with a prismatic calcareous layer[4,5,9]. Both conditions are optimized as ancestral to amniotes in our sample (Fig. 3). The presence of a prismatic layer in extant monotremes influences this optimization (Fig. 3). However, we are missing any data on eggshells in stem mammals, stem amniotes or several early diverging reptile clades[4,8,10]. Two major reptile clades—dinosaurs and lepidosaurs—acquired to different degrees a thin eggshell for a given egg volume (Figs. 2a, 3). These two independent acquisitions, however, occur in eggs of notably different types and may reflect different contexts and selective pressures. Neognath birds present a thicker calcareous layer for a given egg mass than large nonavian dinosaurs (Figs. 2, 3). This is consistent with a previously proposed upper limit for allometric scaling of hard eggshell thickness, owing to tradeoffs between successful hatching, gas exchange, and maintaining the structural integrity of the egg[3]. Conversely, the poorly mineralized eggshell with no prismatic layer found in lepidosaurs has been linked primarily to plasticity in reproductive strategies, in response to new environmental constraints in that clade that facilitated multiple acquisitions of viviparity[18,20].

Antarcticoolithus samples the previously unknown upper limits of egg volume and eggshell thickness in soft-shelled eggs (Figs. 2, 3). Experimental results for similarly structured eggs from extant lepidosaurs had suggested lower thresholds for egg collapse[27]. Its thin calcareous layer and thick, permeable membrana testacea (Fig. 1g, h and Extended Data Figs. 2, 3) may represent a unique tradeoff between

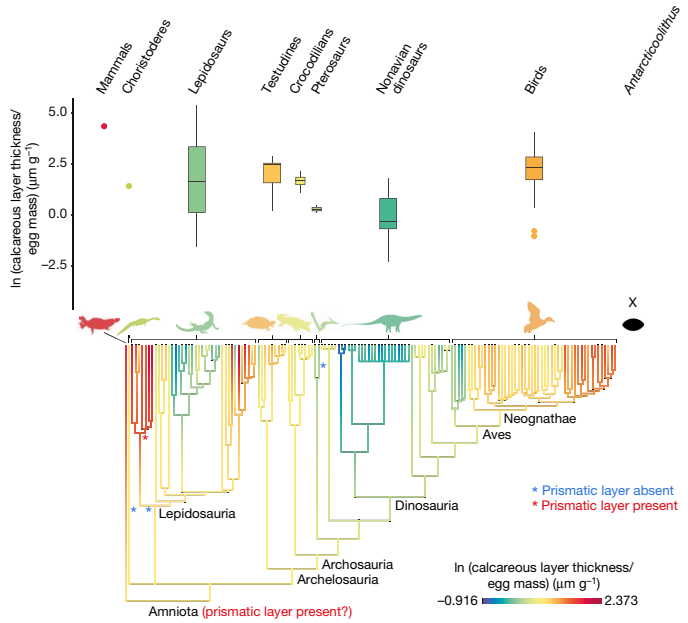

Fig. 3 | Evolution of the relative thickness of the calcareous layer in amniotes. See Supplementary Methods, dataset 2; $n = 148$. The box plots (top) and reconstruction of ancestral state (bottom) use the ratio eggshell thickness/egg mass. Optimized acquisitions and losses of a prismatic calcareous layer are denoted by asterisks. *Antarcticoolithus* ('X') is shown for comparison, but was not included in the state reconstruction owing to its uncertain phylogenetic position. Most amniote hard-shelled eggs show a high relative thickness, except for the eggs of large nonavian dinosaurs and palaeognaths, suggesting a potential allometric upper limit of eggshell thickness. Lepidosaurs display a wide range of relative eggshell thicknesses, consistent with their plasticity in reproductive strategies (Supplementary Discussion). *Antarcticoolithus*, which has the highest absolute thickness among soft-shelled eggs (Fig. 2a), shows the lowest relative thickness among all included amniotes (top). See Extended Data Table 1 for sample size and percentiles of the box plots. Select taxon silhouettes were modified from files under Public Domain licence from phylopic.org (list in the Supplementary Information).

allometric constraints of gigantism and the need for high water intake during development[13,18]. Such large soft-shelled eggs, however, may have been more widespread but so far undersampled[8]. Proteinaceous material, such as eggshell membranes, has been suggested to preserve preferentially in chemically oxidative settings within terrestrial and shallow marine depositional environments[28]. However, the López de Bertodano Formation has been documented as a dominantly euxinic environment[29]. The limited oxidation indicated by the presence of apatite, followed by the net-reducing conditions indicated by the pyrite framboids in *Antarcticoolithus* (Extended Data Figs. 2, 4), may be key to this preservational mode (Supplementary Discussion).

Fossil eggs have a long history of recovery and are comparatively well-represented in the fossil record as fragments[4]. However, soft-shelled eggs, lacking a prismatic layer, have only previously been detailed from lacustrine deposits in China[6,10]. Eggs from archosaurs in terrestrial deposits have recently been reported to be soft-shelled, but whether or not they lacked a prismatic layer is unclear[11] (Supplementary Discussion). Even with these new reports, the absence of recovered eggshell from any stem amniotes and most nonarchosaur reptiles is notable[8]. A systematic bias in terrestrial environments against the preservation of eggs without shell units, similar to *Antarcticoolithus* and the eggs of extant lepidosaurs, may help to explain this pattern of recovery in amniotes.

Online content

Any methods, additional references, Nature Research reporting summaries, source data, extended data, supplementary information, acknowledgements, peer review information; details of author contributions and competing interests; and statements of data and code availability are available at https://doi.org/10.1038/s41586-020-2377-7.

1. Reisz, R. R. The origin and early evolutionary history of amniotes. *Trends Ecol. Evol.* **12**, 218–222 (1997).
2. Blackburn, D. G. Classification of the reproductive patterns of amniotes. *Herpetol. Monogr.* **14**, 371–377 (2000).
3. Birchard, G. F. & Deeming, D. C. Avian eggshell thickness: scaling and maximum body mass in birds. *J. Zool.* **279**, 95–101 (2009).
4. Mikhailov, K. E. Fossil and recent eggshell in amniotic vertebrates: fine structure, comparative morphology and classification. *Spec. Pap. Palaeontol.* **56**, 1–76 (1997).
5. Schleich, H. H. & Kästle, W. *Reptile Egg-Shells: SEM Atlas* (Fischer, 1988).
6. Blackburn, D. G. & Sidor, C. A. Evolution of viviparous reproduction in Paleozoic and Mesozoic reptiles. *Int. J. Dev. Biol.* **58**, 935–948 (2014).
7. Blackburn, D. G. Standardized criteria for the recognition of reproductive modes in squamate reptiles. *Herpetologica* **49**, 118–132 (1993).
8. Sander, P. M. Reproduction in early amniotes. *Science* **337**, 806–808 (2012).
9. Packard, M. J. & DeMarco, V. G. in *Egg Incubation: Its Effects on Embryonic Development in Birds and Reptiles* 53–69 (Cambridge Univ. Press, 1991).
10. Stein, K. et al. Structure and evolutionary implications of the earliest (Sinemurian, Early Jurassic) dinosaur eggs and eggshells. *Sci. Rep.* **9**, 4424 (2019).
11. Norell, M. A. et al. The first dinosaur egg was soft. In *Society of Vertebrate Paleontology 79th Annual Meeting Program and Abstracts* (eds Farke, A., MacKenzie, A. & Miller-Camp, J.) 162 (Soc. Vert. Paleontol., 2019).
12. Lawver, D. R. & Jackson, F. D. A review of the fossil record of turtle reproduction: eggs, embryos, nests and copulating pairs. *Bull. Peabody Museum Nat. Hist.* **55**, 215–236 (2014).
13. Iverson, J. B. & Ewert, M. A. in *Egg Incubation: Its Effects on Embryonic Development in Birds and Reptiles* 87–100 (Cambridge Univ. Press, 1991).
14. Briggs, D. E. G. The role of decay and mineralization in the preservation of soft-bodied fossils. *Annu. Rev. Earth Planet. Sci.* **31**, 275–301 (2003).
15. Grellet-Tinner, G. Membrana testacea of titanosaurid dinosaur eggs from Auca Mahuevo (Argentina): implications for exceptional preservation of soft tissue in Lagerstätten. *J. Vertebr. Paleontol.* **25**, 99–106 (2005).
16. Reguero, M. A. Antarctic paleontological heritage: Late Cretaceous– Paleogene vertebrates from Seymour (Marambio) Island, Antarctic Peninsula. *Adv. Polar Sci.* **30**, 328–355 (2019).
17. Braz, H. B., Almeida-Santos, S. M., Murphy, C. R. & Thompson, M. B. Uterine and eggshell modifications associated with the evolution of viviparity in South American water snakes (*Helicops* spp.). *J. Exp. Zool. B Mol. Dev. Evol.* **330**, 165–180 (2018).
18. Andrews, R. M. & Mathies, T. Natural history of reptilian development: constraints on the evolution of viviparity. *Bioscience* **50**, 227–238 (2000).
19. Simões, T. R. et al. The origin of squamates revealed by a Middle Triassic lizard from the Italian Alps. *Nature* **557**, 706–709 (2018).
20. Shine, R. Life-history evolution in reptiles. *Annu. Rev. Ecol. Evol. Syst.* **36**, 23–46 (2005).
21. Meiri, S., Feldman, A. & Kratochvíl, L. Squamate hatchling size and the evolutionary causes of negative offspring size allometry. *J. Evol. Biol.* **28**, 438–446 (2015).
22. Shine, R. Relative clutch mass and body shape in lizards and snakes: is reproductive investment constrained or optimized? *Evolution* **46**, 828–833 (1992).
23. Zhang, L., Guo, K., Zhang, G.-Z., Lin, L.-H. & Ji, X. Evolutionary transitions in body plan and reproductive mode alter maintenance metabolism in squamates. *BMC Evol. Biol.* **18**, 45 (2018).
24. O'Keefe, F. R. & Chiappe, L. M. Viviparity and K-selected life history in a Mesozoic marine plesiosaur (Reptilia, Sauropterygia). *Science* **333**, 870–873 (2011).
25. Lovegrove, B. G. A phenology of the evolution of endothermy in birds and mammals. *Biol. Rev. Camb. Philos. Soc.* **92**, 1213–1240 (2017).
26. Bernard, A. et al. Regulation of body temperature by some Mesozoic marine reptiles. *Science* **328**, 1379–1382 (2010).
27. Sinervo, B. & Licht, P. Proximate constraints on the evolution of egg size, number, and total clutch mass in lizards. *Science* **252**, 1300–1302 (1991).
28. Wiemann, J. et al. Fossilization transforms vertebrate hard tissue proteins into N-heterocyclic polymers. *Nat. Commun.* **9**, 4741 (2018).
29. Schoepfer, S. D., Tobin, T. S., Witts, J. D. & Newton, R. J. Intermittent euxinia in the high-latitude James Ross Basin during the latest Cretaceous and earliest Paleocene. *Palaeogeogr. Palaeoclimatol. Palaeoecol.* **477**, 40–54 (2017).

Publisher's note Springer Nature remains neutral with regard to jurisdictional claims in published maps and institutional affiliations.

© The Author(s), under exclusive licence to Springer Nature Limited 2020

Reporting summary

Further information on research design is available in the Nature Research Reporting Summary linked to this paper.

Data availability

CT scan data are available from Open Science Framework at https://osf.io/gx8fq/. All other data generated or analysed here are included in the Supplementary Information (Supplementary Tables 1–3). The code used for all statistical analyses is available on GitHub at https://github.com/LucasLegendre/Antarcticoolithus_project.

Acknowledgements We thank J. Singh, T. Etzel, G. Rojas, V. Lynch and N. Miller for technical assistance with thin-sectioning, scanning electron microscopy, CT scanning, X-ray diffraction and inductively coupled plasma mass spectrometry, respectively (Supplementary Methods); L. Scheinberg (California Academy of Sciences), D. Kizirian (American Museum of Natural History), T. LaDuc and K. Bader (University of Texas at Austin) for specimen access; C. Gutstein and R. F. Jimenez for assistance with fossil collection and sampling; and M. Cloos, R. Martindale, C. Kerans, C. Torres, M. Leppe, N. Crouch and S. Hood for discussions. Select taxon silhouettes in Figs. 2, 3 were modified from files under Public Domain licence from phylopic.org. This work was supported by a grant to the University of Texas at Austin from the Howard Hughes Medical Institute through the Science Education Program (GT10473 to J.A.C. and L.J.L.) and by an ANID-PIA Anillo grant (ACT172099 to D.R.-R., R.A.O. and A.O.V.).

Author contributions J.A.C., D.R.-R. and L.J.L. conceived the study; D.R.-R. and R.A.O. collected the specimen; D.R.-R., R.A.O. and A.O.V. prepared the specimen and contributed to its description; L.J.L. collected the data and performed experiments and statistical analyses; S.N.D. sampled the specimen and contributed to its description; G.M.M. contributed to the description and line drawings of the specimen; L.J.L. and J.A.C. wrote the paper; all authors discussed and contributed to the final draft of the manuscript.

Competing interests The authors declare no competing interests.

Additional information
Supplementary information is available for this paper at https://doi.org/10.1038/s41586-020-2377-7.
Correspondence and requests for materials should be addressed to L.J.L. or J.A.C.
Peer review information *Nature* thanks Johan Lindgren, Jasmina Wiemann and the other, anonymous, reviewer(s) for their contribution to the peer review of this work.
Reprints and permissions information is available at http://www.nature.com/reprints.

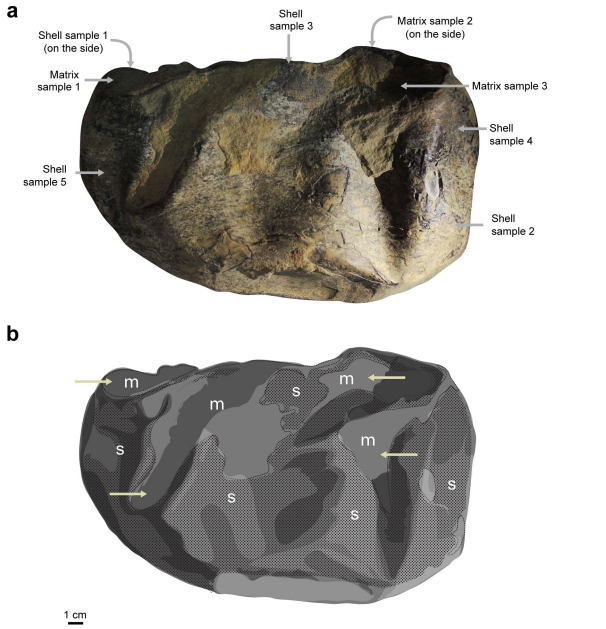

Extended Data Fig. 1 | The holotype specimen of *A. bradyi* in bottom view. This side of the specimen, deeply flattened, is referred to as the inferior side in the Supplementary Discussion. **a**, Photograph of SGO.PV 25.400, showing the sampling locations of eggshell and sediment matrix fragments used for experiments (Supplementary Methods and Extended Data Fig. 4). **b**, Line drawing of **a**, showing the relative arrangement of the eggshell (s) and the infilling sediment matrix (m) at the surface of the specimen. The matrix is visible through large creases (yellow arrows), corresponding to zones of local collapsing and infolding of the eggshell.

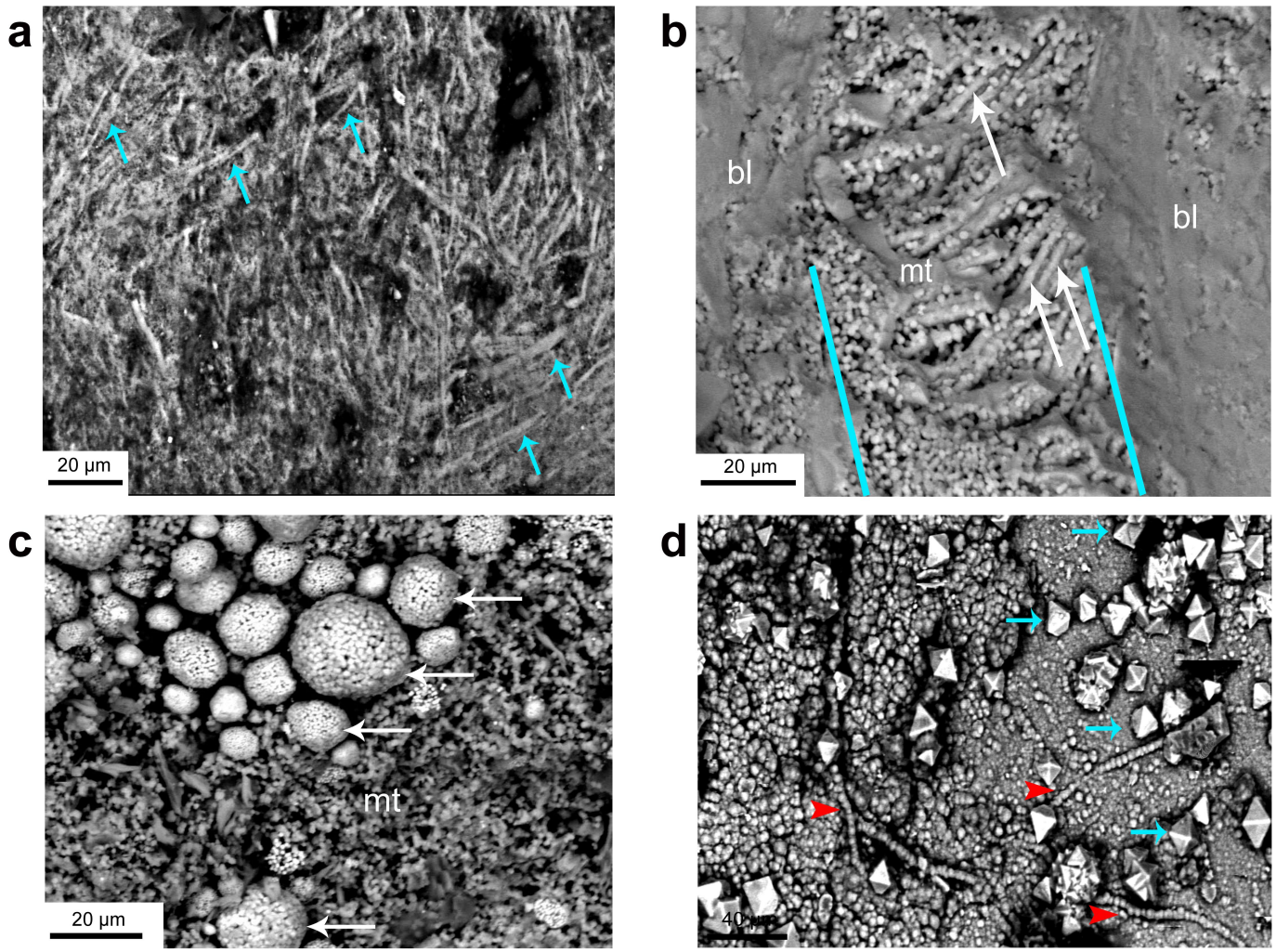

Extended Data Fig. 2 | Scanning electron microscopy images of the eggshell of *A. bradyi*. **a**, The outer surface of the membrana testacea (mt) shows intersecting fibres (blue arrows). **b**–**d**, The smooth inner surface of the eggshell, identified as the boundary layer (bl in **b**), can be locally broken off, showing the structures consistent with remnants of protein fibrils seen in the membrana testacea of extant taxa (arrows in **b**, red triangles in **d**), and revealing an underlying, dense, irregular globular pattern, identified as part of the membrana testacea (**b**, **c**). Pyrite crystals, present in most samples within the membrana testacea, show a framboidal (arrows in **c**) or octahedral (blue arrows in **d**) structure. Eggshell sampling locations: 2 (**c**) and 4 (**a**, **b**, **d**) in Extended Data Fig. 1. Further detail on the eggshell structure and methods is found in the Supplementary Methods, Supplementary Discussion, Fig. 1 and Extended Data Figs. 1, 3, 4.

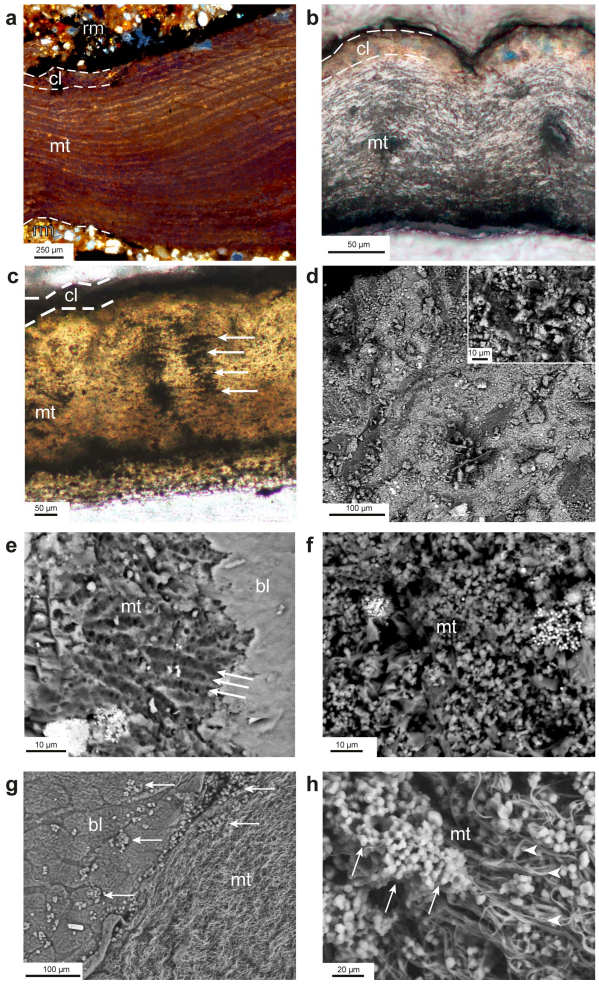

Extended Data Fig. 3 | Microstructure of *A. bradyi* and several species of extant lepidosaurs. a–**c**, Observed under an optical microscope; **d**–**h**, observed by scanning electron microscopy (SEM). mt, membrana testacea; bl, boundary layer; cl, calcareous layer; rm, rock matrix. **a**–**c**, Histological thin sections of the eggshell of *Antarcticoolithus* (**a**), a common kingsnake (*Lampropeltis getula*, **b**) and a gold tegu (*Tupinambis teguixin*, **c**), showing their similarities in microstructure. Dashed lines in **a** delimit the inner and outer surface of the eggshell, as well as the less-obvious boundary between layers in the shell. Arrows in **c** indicate layering between protein fibrils, which is slightly less conspicuous than in **a**, **b**. **d**, Surface of the sediment matrix of *Antarcticoolithus*, showing a granular texture distinct from that of the eggshell (see inset at top right corner). **e**, **f**, Inner surface of the eggshell of *Antarcticoolithus*, locally showing fibrous structures (arrows in **e**) that might correspond to protein fibrils, and a dense globular pattern (**f**). **g**, **h**, Inner surface of the eggshell of two extant lepidosaurs: an ornate tree lizard (*Urosaurus ornatus*, **g**) and a common side-blotched lizard (*Uta stansburiana*, **h**). The boundary layer is partially missing, revealing the protein fibrils (arrowheads in **h**) in the membrana testacea. Calcified globules (arrows in **g**, **h**) are also present among the fibrillar structures, with some being isolated and deposited at the surface of the boundary layer (probably during mounting before SEM sampling). Sampling locations for *Antarcticoolithus* (from Extended Data Fig. 1): matrix sample, 3 (**d**); eggshell samples, 2 (**e**, **f**) and 3 (**a**). See also Fig. 1, Extended Data Figs. 1, 2, Supplementary Methods and Supplementary Discussion.

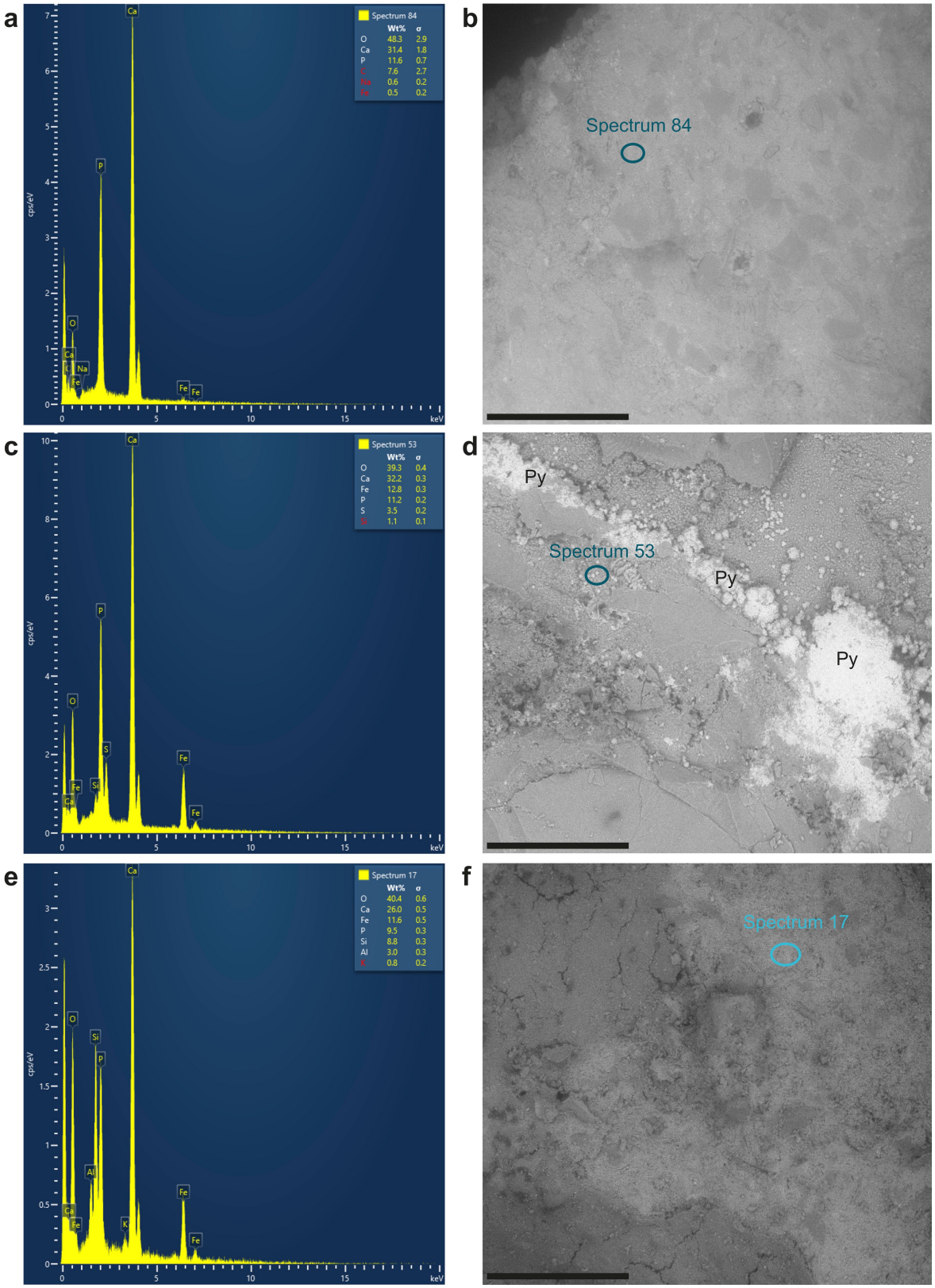

Extended Data Fig. 4 | Spectra for the eggshell and matrix of *A. bradyi*. **a**, **c**, **e**, Spectra obtained using energy-dispersive X-ray spectroscopy; cps, counts per second. **b**, **d**, **f**, Corresponding sampling locations on the specimen, indicated by blue circles. **a**, **b**, Shell sample 3 (inner surface), showing high amounts of calcium (Ca), oxygen (O) and phosphorus (P), characteristic of apatite. **c**, **d**, Shell sample 4 (inner surface), showing apatite as well as iron (Fe) and sulfur (S), indicating the presence of pyrite crystals (labelled Py in **d**). **e**, **f**, Matrix sample 3 (outer surface), showing a combination of apatite and silicates, the latter containing silicon (Si) and oxygen. Traces of potassium (K), aluminium (Al) and sodium (Na) can also be detected. Scale bar, 500 µm. See Extended Data Fig. 1 for sampling locations.

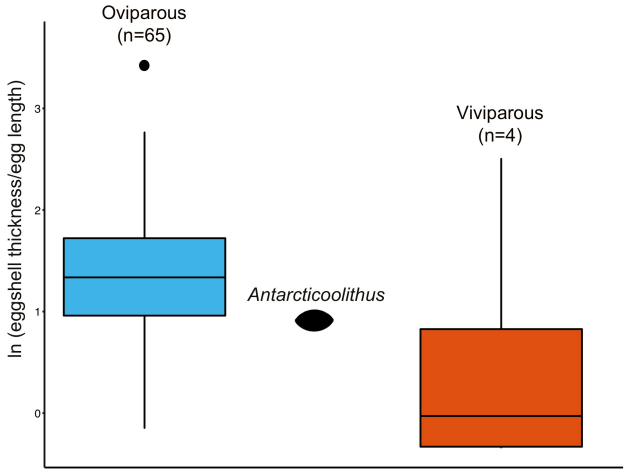

Extended Data Fig. 5 | Distribution of eggshell thickness corrected for egg length for extant lepidosaurs in our sample and for *A. bradyi*. The extant lepidosaurs are listed in Supplementary Methods, dataset 1. *Antarcticoolithus* is represented by a black ovoid; its eggshell thickness/egg length (ET/L) ratio is intermediate between the averages obtained for oviparous and viviparous lepidosaurs. A phylogenetic one-way analysis of variance performed on oviparous and viviparous taxa in our sample identified a significant difference in ET/L ratio between the two groups ($F = 6.076968$; $P = 0.007$) (Supplementary Methods). The small sample size of viviparous species is due to the scarcity of studies on eggshell thickness in viviparous lepidosaurs. Percentiles of box plots are available in Extended Data Table 1. See also Supplementary Discussion and Supplementary Table 1.

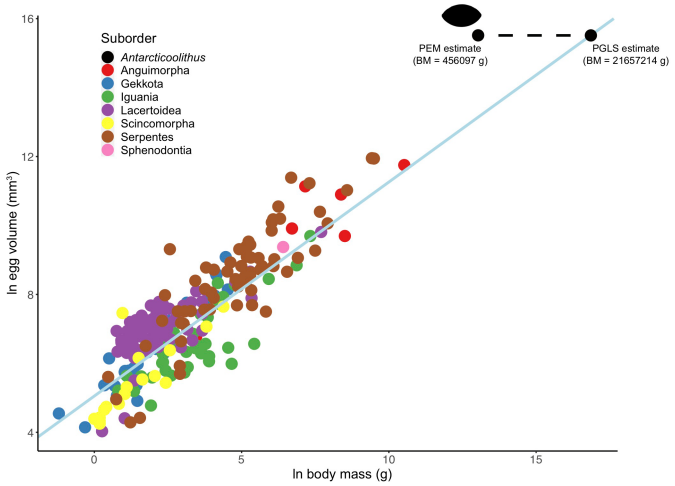

Extended Data Fig. 6 | Scaling of egg volume with body mass for our sample of extant lepidosaurs. See dataset 1 in the Supplementary Methods ($n = 241$); each clade is labelled. The regression line corresponds to a PGLS fit ($r^2 = 0.6851$; $P < 2.2 \times 10^{-16}$). For *Antarcticoolithus*, estimates of body mass (BM) from both PEMs and PGLS are provided. The PEM estimate is very low for a giant marine reptile of more than 10 m in length (see text), which is probably due to the lack of taxa within the 10^6 g order of magnitude usually inferred for large marine reptiles. Conversely, the PGLS estimate is surprisingly high, which might be linked to the large gap in egg-volume values between *Antarcticoolithus* and extant lepidosaurs, as suggested by the similar results we obtained with body-length estimations (Fig. 2, Supplementary Methods and Supplementary Table 1).

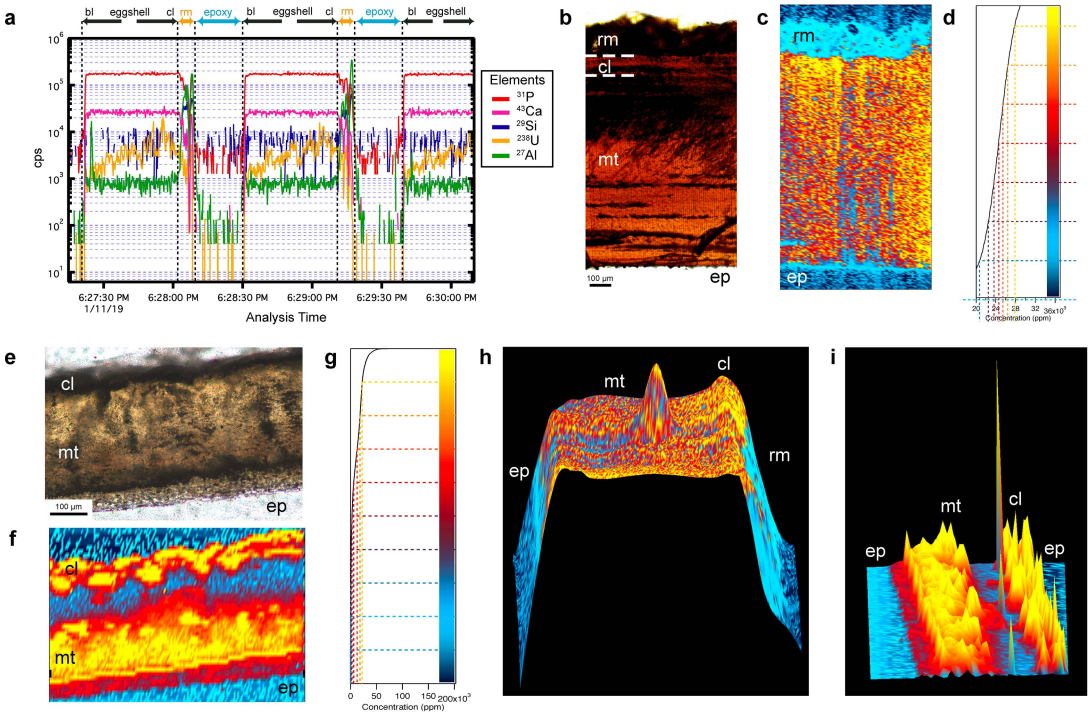

Extended Data Fig. 7 | Element mapping of the eggshell of *A. bradyi* and extant lepidosaurs, obtained using inductively coupled plasma mass spectrometry. a, Counts per second (cps) for major elements in the eggshell of *A. bradyi*. bl, boundary layer; cl, calcareous layer; rm, rock matrix. Two and a half cycles are shown, each cycle corresponding to laser ablation and measurement of elemental relative density through the whole eggshell from the inside to the outside, through an outer layer of sediment, and through the surrounding epoxy of the thin section. Calcium and phosphorus are present at high concentrations in the eggshell, and silicon and aluminium are more prominent in the sediment; uranium, an element present in low amounts in both shell and sediment, is shown for comparison. **b**–**d**, Eggshell thin section of *A. bradyi* (**b**), with corresponding element map (**c**) and scale (**d**) showing relative amounts of calcium (^{43}Ca) in the eggshell. Calcium is abundant in the eggshell, but absent in the outer layer of sediment (rm); ep, epoxy resin. **e**–**g**, Eggshell thin section of a gold tegu (*T. teguixin*; **e**), with corresponding element map (**f**) and scale (**g**) showing relative amounts of calcium (^{43}Ca) in the eggshell. Calcium is mostly present in the calcareous layer, but also featured in the lower portion of the membrana testacea, probably through calcite globules, as documented in many lepidosaur species (see, for example, ref. [5]). **h**, **i**, Relative density maps for calcium (^{43}Ca) in *A. bradyi* (**h**) and *T. teguixin* (**i**), corresponding to side views of the maps shown in **c** and **f**, respectively. Peaks indicate a high amount of calcium, and flat surfaces and depressions indicate a lower amount. In both maps, the calcareous layer tends to show the highest amount, suggesting its preservation in *A. bradyi* and the general structural similarity between the two thin sections. Both maps present a single, very high peak in their centre, which could also be identified in all element maps for each section, and most probably corresponds to a contamination artefact. Colour gradients for **h** and **i** are the same as in **d** and **g**, respectively. See also Supplementary Methods and Supplementary Discussion.

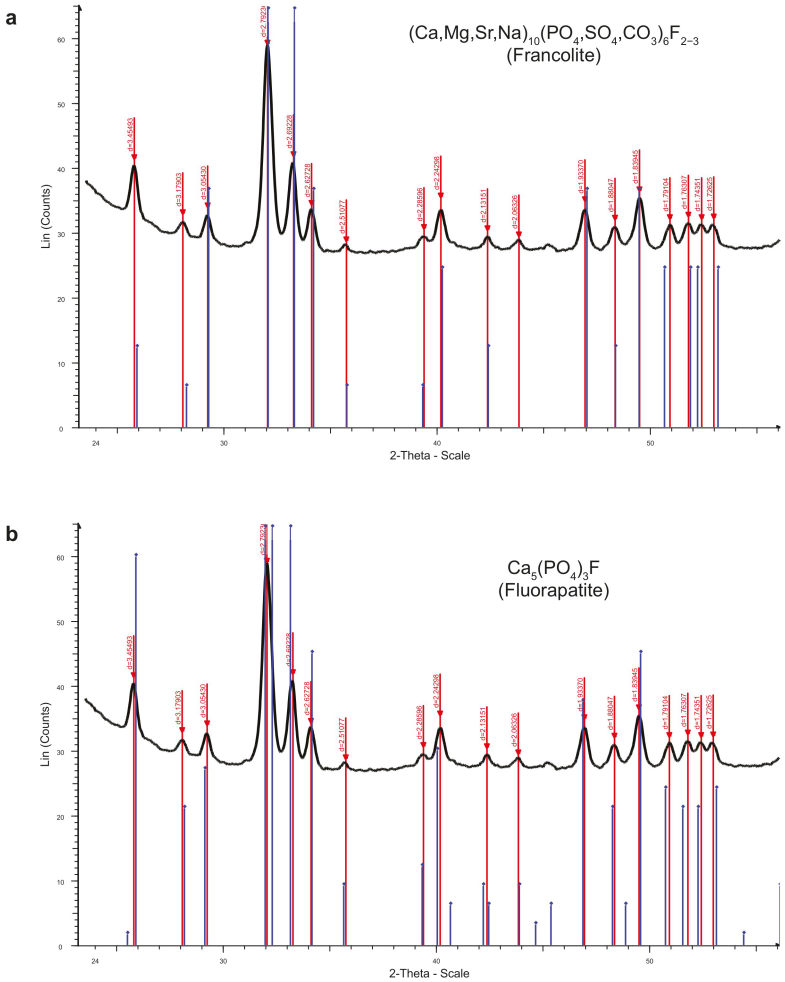

Extended Data Fig. 8 | Powder X-ray diffraction spectra of the eggshell of *A. bradyi*. The two best matches for these spectra are francolite (**a**) and fluorapatite (**b**). Lin, linear intensity. See the Supplementary Methods for a detailed description of the protocol, and Supplementary Discussion for an interpretation of the results.

Extended Data Table 1 | Sample sizes and percentiles of box plots

Figure 3						
Clade	**Sample size**	**Minimum**	**First quartile**	**Median**	**Third quartile**	**Maximum**
Lepidosaurs	38	-1.4307461	0.2392498	1.7701329	3.4510661	5.4647026
Chelonians	9	0.2636401	1.6216397	2.5162801	2.5794171	2.9038769
Crocodilians	8	1.1282254	1.5449861	1.7324607	1.9034789	2.2137481
Pterosaurs	2	0.2876821	0.3729137	0.4581454	0.5433770	0.6286087
Non-avian dinosaurs	39	-2.1102132	-0.4793495	-0.1364957	0.9978001	1.9902104
Birds	50	0.4296871	1.8265428	2.4120341	2.9394662	4.1207778
Extended Data Figure 5						
Group	**Sample size**	**Minimum**	**First quartile**	**Median**	**Third quartile**	**Maximum**
Oviparous	65	-0.1251631	0.9808293	1.35720692	1.7429693	2.784423
Viviparous	4	-0.3462762	-0.3308263	-0.02868824	0.8270896	2.503459

Relates to Fig. 3 and Extended Data Fig. 5. Values of percentiles correspond to relative eggshell thickness, estimated as ln(eggshell thickness/egg mass) for Fig. 3, and as ln(eggshell thickness/egg length) for Extended Data Fig. 5. See also Supplementary Methods.

nature research

Corresponding author(s): Lucas J. Legendre, Julia A. Clarke

Last updated by author(s): Mar 10, 2020

Reporting Summary

Nature Research wishes to improve the reproducibility of the work that we publish. This form provides structure for consistency and transparency in reporting. For further information on Nature Research policies, see Authors & Referees and the Editorial Policy Checklist.

Statistics

For all statistical analyses, confirm that the following items are present in the figure legend, table legend, main text, or Methods section.

n/a	Confirmed
☐	☒ The exact sample size (*n*) for each experimental group/condition, given as a discrete number and unit of measurement
☐	☒ A statement on whether measurements were taken from distinct samples or whether the same sample was measured repeatedly
☐	☒ The statistical test(s) used AND whether they are one- or two-sided *Only common tests should be described solely by name; describe more complex techniques in the Methods section.*
☐	☒ A description of all covariates tested
☐	☒ A description of any assumptions or corrections, such as tests of normality and adjustment for multiple comparisons
☐	☒ A full description of the statistical parameters including central tendency (e.g. means) or other basic estimates (e.g. regression coefficient) AND variation (e.g. standard deviation) or associated estimates of uncertainty (e.g. confidence intervals)
☐	☒ For null hypothesis testing, the test statistic (e.g. *F*, *t*, *r*) with confidence intervals, effect sizes, degrees of freedom and *P* value noted *Give P values as exact values whenever suitable.*
☒	☐ For Bayesian analysis, information on the choice of priors and Markov chain Monte Carlo settings
☒	☐ For hierarchical and complex designs, identification of the appropriate level for tests and full reporting of outcomes
☐	☒ Estimates of effect sizes (e.g. Cohen's *d*, Pearson's *r*), indicating how they were calculated

Our web collection on statistics for biologists contains articles on many of the points above.

Software and code

Policy information about availability of computer code

Data collection	Original measurements for our Datasets 1 and 2 were taken on pictures using ImageJ 2.0.0 (Open Source) and compiled in Microsoft Excel 16.16.14 (Microsoft Corporation, WA, US). The phylogenetic trees used in the analyses were compiled in Mesquite 3.6 (Open Source). SEM and EDS images were collected using JSM-6490LV (JEOL, Ltd., Japan) and AZtecOne 3.3 (Oxford Instruments, UK). XRD data were acquired using Rigaku R-AXIS SPIDER (Applied Rigaku Technologies, TX, USA) and analyzed using EVA (Bruker Corporation, MA, USA). ICP-MS data were acquired using Agilent 7500ce ICP-MS (Agilent Technologies, Inc., CA, USA) and analyzed using Iolite v3.1 (University of Melbourne) and IGOR Pro 8 (WaveMetrics, OR, USA). All image were compiled and edited using Adobe Photoshop CS6 13.0 and Illustrator CS6 16.0.0 (Adobe Inc., CA, US). CT scan images were analyzed in Avizo 2019.1 (Thermo Fischer Scientific, MA, USA). All additional information is available in the Supplementary Methods.
Data analysis	All analyses were performed in R 3.6.2 (Open Source), using specific packages available on the online CRAN repository. Specific R packages used for analyses are: ape v5.3 (Paradis et al., 2019), nlme v3.1-144 (Pinheiro et al., 2020), AICcmodavg v2.2-2 (Mazerolle, 2019), phytools v0.6-99 (Revell, 2019), MPSEM v0.3-6 (Guénard, 2019), and phylopath v1.1.2 (van der Bijl, 2019).

For manuscripts utilizing custom algorithms or software that are central to the research but not yet described in published literature, software must be made available to editors/reviewers. We strongly encourage code deposition in a community repository (e.g. GitHub). See the Nature Research guidelines for submitting code & software for further information.

Data

Policy information about availability of data

All manuscripts must include a data availability statement. This statement should provide the following information, where applicable:

- Accession codes, unique identifiers, or web links for publicly available datasets
- A list of figures that have associated raw data
- A description of any restrictions on data availability

All measurements collected for this study are available as individual datasets, labelled Supplementary Tables 1, 2, and 3 in the Supplementary Information of this

paper.

Field-specific reporting

Please select the one below that is the best fit for your research. If you are not sure, read the appropriate sections before making your selection.

☐ Life sciences ☐ Behavioural & social sciences ☒ Ecological, evolutionary & environmental sciences

For a reference copy of the document with all sections, see nature.com/documents/nr-reporting-summary-flat.pdf

Ecological, evolutionary & environmental sciences study design

All studies must disclose on these points even when the disclosure is negative.

Study description	This study describes a new fossil egg taxon from Antarctica, and examines its characteristics in relations with other amniote eggs. Dataset of egg measurements were compiled from new specimens and the literature to perform such comparisons (see below).
Research sample	The research sample includes two datasets of (respectively) 259 lepidosaur species and 148 amniote species (some of which are included in both datasets; see Supplementary Tables 1–3), representing the vertebrate clades Lepidosauria and Amniota, respectively. A detailed list of all specimens collected for this study, all species used in this study, and all references in the literature from which data were collected, is available in Supplementary Tables 1–3 and associated references.
Sampling strategy	Lepidosaur egg measurements are scarcely available in existing literature. We performed a comprehensive review of available studies on quantitative analyses of such measurements in lepidosaurs to build a preliminary dataset, and completed it with measurements assembled from research collections in the United States (AMNH, CAS, UT Austin). This represents the largest existing dataset, and the only one including species of each major clade of lepidosaurs, for extant soft-shelled egg measurements. Also see Supplementary Methods.
Data collection	All data was collected at UT Austin by L. J. Legendre. Specimens of extant lepidosaur eggs collected for this study were loaned from their original host institutions by curators of corresponding research collections (see Acknowledgments, Supplementary Table 2). Samples of the eggshell of the new specimen described as Antarcticoolithus bradyi were collected by D. Rubilar-Rogers and S. N. Davis in the Museo Nacional de Historia Natural (Santiago, Chile). Analyses of eggshell microstructure were performed at the Jackson School of Geosciences, UT Austin, TX, USA (see Supplementary Methods).
Timing and spatial scale	Specimens were obtained, sampled, processed, scanned, and imaged over a period of six months (January–June 2019) at the Jackson School of Geosciences, UT Austin, TX, USA (see Supplementary Methods).
Data exclusions	All data collected were included in the final sample used in this study and available as Supplementary Information (Supplementary Tables 1–3)
Reproducibility	When available, several extant lepidosaur eggs, and/or several eggshell fragments for each egg were thin-sectioned and looked at using light microscopy and SEM (see Supplementary Methods; Supplementary Table 2). For Antarcticoolithus bradyi, multiple eggshell fragments were sampled and analysed for each procedure (Supplementary Methods; Extended Data Figure 1). The structures described and the measurements obtained for each fragment were consistent for each sampled species in the dataset (Fig. 1, 2; Supplementary Methods; Extended Data Fig. 1, 2; Supplementary Table 1 –3).
Randomization	We tested the allometric scaling relationships for each of the two samples, to compare Antarcticoolithus to both other soft-shelled eggs (Dataset 1) and other amniotic eggs in general (Dataset 2). We also separated Dataset 1 in two groups based on reproductive strategy (oviparity/viviparity) to test for a significant difference in eggshell thickness between them using phylogenetic ANOVAs (see Supplementary Methods). No other subset of the data were performed.
Blinding	Not applicable (this study did not include any comparison between a test group and a control group; see Supplementary Methods).

Did the study involve field work? ☐ Yes ☒ No

Reporting for specific materials, systems and methods

We require information from authors about some types of materials, experimental systems and methods used in many studies. Here, indicate whether each material, system or method listed is relevant to your study. If you are not sure if a list item applies to your research, read the appropriate section before selecting a response.

Materials & experimental systems

n/a	Involved in the study
☒	☐ Antibodies
☒	☐ Eukaryotic cell lines
☐	☒ Palaeontology
☒	☐ Animals and other organisms
☒	☐ Human research participants
☒	☐ Clinical data

Methods

n/a	Involved in the study
☒	☐ ChIP-seq
☒	☐ Flow cytometry
☒	☐ MRI-based neuroimaging

Palaeontology

Specimen provenance	The specimen SGO.PV 25.400 was recovered in siltstone sediments in the Late Maastrichtian of Seymour Island, Antarctica (López de Bertodano Formation) during the 47th Antarctican Scientific Expedition (2011), organized by the Chilean Antarctic Institute (INACH). The specimen was collected with permits in accordance with the Antarctic Treaty, provided by the Chilean Antarctic Institute Authorities (permits: INACH 065-2011) to Anillo de Ciencia Antártica (ACT-105, Conicyt-Chile). Logistical support for fieldwork was provided by INACH. Research on the fossil once reposited in Chile was funded by an Anillo grant (CONICYT-PIA: National Commission for Scientific and Technological Research Program of Associative Investigation; ACT172099).
Specimen deposition	Specimen SGO.PV 25.400 is permanently reposited at the Museo Nacional de Historia Natural, Santiago, Chile.
Dating methods	Not applicable (no new dates were estimated for this study).

☐ Tick this box to confirm that the raw and calibrated dates are available in the paper or in Supplementary Information.